Liquid Crystals
Publication details, including instructions for authors and subscription information:
http://www.informaworld.com/smpp/title~content=t713926090

Mesomorphic chiral non-symmetrical dimers: synthesis and characterization

C. V. Yelamaggad[a]; G. Shanker[a]
[a] Centre for Liquid Crystal Research, Jalahalli, Bangalore 560 013, India

To cite this Article Yelamaggad, C. V. and Shanker, G.(2007) 'Mesomorphic chiral non-symmetrical dimers: synthesis and characterization', Liquid Crystals, 34: 7, 799 — 809
To link to this Article: DOI: 10.1080/02678290701478921
URL: http://dx.doi.org/10.1080/02678290701478921

Liquid Crystals, Vol. 34, No. 7, July 2007, 799–809

Mesomorphic chiral non-symmetrical dimers: synthesis and characterization

C.V. YELAMAGGAD* and G. SHANKER
Centre for Liquid Crystal Research, Jalahalli, Bangalore 560 013, India

(*Received 25 January 2007; accepted in revised form 14 May 2007*)

The preparation and phase transitional properties of several optically active non-symmetrical dimers are reported. Two types of dimeric mesogens formed by covalently combining pro-mesogenic cholesterol with either phenyl 4-cyanobenzoate (polar) or phenyl *trans*-4-pentylcyclohexanecarboxylate (apolar) cores in an end-to-end fashion through an ω-oxyalkanoyl spacer were investigated. The phase behaviour of these two types of dimers differs, indicating that the nature and extent of mesomorphism are sensitive to the structure of the mesogen attached to the cholesterol. However, within the series, the spacer parity greatly influences the clearing temperatures of the materials, as expected. In general, all the compounds display an enantiotropic chiral nematic (N*) phase; several of them also stabilize smectic and/or twist grain boundary phases. The optical properties of the N* phase of all the compounds were investigated with the aid of both UV–visible and chiroptical spectroscopic techniques. These complementary studies revealed that the dimers exhibit an odd–even effect in the wavelength of selective reflection, with even-parity members having higher values, similar to previous reports. The chiroptical spectroscopy indicated that the N* pitch is right-handed for all the investigated dimers, which is in accordance with the fact that most steroidal esters are right-handed.

1. Introduction

In recent years, mesomorphic non-symmetrical dimers possessing two chemically dissimilar anisometric segments interlinked through a flexible spacer have been emerged as the exciting synthetic targets for chemists since they display a rich phase behaviour [1]. In particular, optically active dimers, formed by covalently linking pro-mesogenic cholesterol with an aromatic rod-like core through an alkylene spacer, exhibit a range of unique liquid crystalline behaviour [2–22] originating from the complex intermolecular interactions among the cores, terminal chain and the spacer. The initial interest in such dimers originated from the discovery by Jin and co-workers [2] that a dimer consisting of cholesterol and Schiff base entities interlinked via an 5-oxypentanoyl spacer displays a rich polymesomorphic sequence including an incommensurate smectic A (SmA_{ic}) phase (see following section for details). Since then, in addition to our group [16–19], Jin and co-workers [2–10], Marcelis *et al.* [11–14] and Tamaoki's group [22] have been focusing on the design and synthesis of such dimers, primarily to understand the correlation between molecular structure and mesomorphic behaviour. Thus, it is very apparent from the accumulated results that the cholesterol-based dimers themselves are of significant interest in their own right as they display liquid crystal (LC) properties that are attractive for fundamental research [2–22]. Importantly, the molecular architecture of such dimers offers a unique and practical way to design multi-functional systems through the appropriate selection of mesogens [22].

Nonetheless, the clear understanding of the correlation between the overall molecular structure and thermal properties of these dimers is still very much in its infancy; the task seems to be tedious, as several structural factors are involved. However, one of the general and fascinating features of such dimers is the critical dependence of their phase behaviour on the parity (i.e. odd or even) and the chemical nature of linking groups between the spacer. Indeed, the chemical nature of the rod-like (non-cholesteryl) mesogenic segment (including terminal moiety it possesses) also influences the transitional properties of these dimers. For example, as mentioned above, the molecular structure of the aromatic core is imperative for the occurrence of an incommensurate phase than for the appearance of other frustrated mesophases, i.e. the blue phases (BP), the twist grain boundary (TGB) phase and the chiral smectic C (SmC*)

*Corresponding author. Email: Yelamaggad@gmail.com

Liquid Crystals
ISSN 0267-8292 print/ISSN 1366-5855 online © 2007 Taylor & Francis
http://www.tandf.co.uk/journals
DOI: 10.1080/02678290701478921

phase [3–5, 16–19]. However, in the context of smectic A (SmA) behaviour and its structural (periodicity) modification in such dimers, some hints are available. An aromatic core possessing either a chiral tail [17, 19] or perfluorinated tail seems to favour the formation of the SmA phase [9, 10, 20] solely. Furthermore, the fascinating structural variations of the SmA phase depend on the relative lengths of the spacer and terminal chains as well as on the nature of the aromatic core to some extent. For example, dimers with long spacers exhibit an intercalated smectic A (SmA_c) phase with $d/L=0.5$, where d is the layer spacing derived from the X-ray diffraction (XRD) studies and L is the estimated all-*trans* molecular length, whereas if the spacer is shorter than the terminal chain then a monolayer SmA phase ($d/L=1$) is formed [6, 7, 13, 17, 19]. The aforementioned novel incommensurate smectic A (SmA_{ic}) phase featuring the coexistence of competing periodicities is stabilized in Schiff's bases when the lengths of spacer and terminal tail are nearly equal [2–4]. For the dimers with an electron withdrawing terminal group the occurrence of an interdigitated SmA (SmA_d) phase ($d/L=1.5$–1.8) composed of bimolecular antiparallel pairs has been evidenced in recent investigations by several groups [7, 13].

Thus, the examples reported clearly illustrate the complex interplay of the different segments in the mesophase formation of these dimers and the need for the synthesis of new compounds. Indubitably, there is considerable scope in this research area to derive such systems with diverse molecular architecture that possibly facilitates to reveal their general phase behaviour. In continuation of our efforts to understand the relationship between molecular structural features and mesomorphic properties, a study was undertaken wherein two different rod-like cores, i.e. phenyl 4-cyanobenzoate and phenyl *trans*-4-pentylcyclohexanecarboxylate, were chosen to individually combine with cholesterol via a ω-oxyalkanoyl spacer varying in its parity and length. In this paper we report the synthesis and mesomorphism of two types of dimers, the cholesteryl ω-[4-(4-cyanobenzoyloxy)-phenoxy] alkanoates and cholesteryl ω-[4-(*trans*-1,4-butylcyclohexanoyloxy)phenoxy]alkanoates. The acronyms used to symbolize these dimers are **I-n** and **II-n**, respectively, where **n** signifies the total number of carbon atoms in the spacer obtained by including the number of carbon atoms in **m**, the methylene units and also that of the carbonyl group.

2. Experimental

2.1. *General*

Reagent-grade dichloromethane was obtained from a local source and distilled over calcium hydride prior to use. The other reagents were purchased from either Aldrich or local companies, and were used as received. Thin layer chromatography (TLC) was performed on aluminium sheets pre-coated with silica gel (Merck, Kieselgel 60, F_{254}). The intermediates and target compounds were purified by column chromatography using either silica gel (400 mesh) or neutral aluminium oxide as a stationary phase. The UV–visible spectra were recorded using a Perkin Elmer Lambda 20 UV-Vis spectrometer. FT-IR spectra were recorded on a Perkin Elmer Spectrum 1000 FT-IR spectrophotometer using KBr disks. NMR spectra were recorded on a Bruker AMX-400 spectrometer (operating at 400 MHz) in $CDCl_3$ with $SiMe_4$ (TMS) as an internal standard. The chemical shifts are reported in parts per million (ppm) relative to TMS. Mass spectra were recorded on a Jeol-JMS-600H spectrometer in FAB^+ mode using 3-nitrobenzyl alcohol as a liquid matrix. Elemental analyses were performed using Eurovector model EA 3000 CHNS analyser. Circular dichroism (CD) measurements were recorded with the aid of Jasco J-810 spectropolarimeter. The identification of the mesophases and the transition temperatures of the compounds were determined using a polarizing optical microscope (POM) (Leitz DMRXP or Leica DMLP) in conjunction with a programmable hot stage (Mettler FP90). The transition temperatures and associated enthalpies were determined by differential scanning calorimeter (DSC) (Perkin Elmer DSC7).

2.2. *Synthesis and structural characterization*

The dimers and their requisite precursors were prepared following the synthetic route described in scheme 1. Cholesteryl ω-bromoalkanoates (**1a**–**d**) were obtained by esterification of alkanoyl chlorides with cholesterol using pyridine as the base [23]. The key intermediates, cholesteryl ω-(4-hydroxyphenoxy)alkanoates (**2a**–**d**) were prepared by treating hydroquinone (in large excess) with cholesteryl ω-bromoalkanoates in the presence of a mild base in DMF. Finally chiral dimers were obtained by esterification between the individual phenols (**2a**–**d**) and 4-cyanobenzoic acid or *trans*-4-pentyl-cyclohexanecarboxylic acid in the presence of dicyclohexylcarbodiimide (DCC) and 4-(*N*,*N*-dimethylamino)pyridine (DMAP) using dichloromethane. The molecular structures of the intermediates and nonsymmetric dimers were confirmed with help of spectroscopic (FT-IR, NMR, and MS) and elemental analyses. The characterization data of all the intermediates and dimers were found to be in agreement with their structures.

2.2.1. General procedure for dimer preparation. A mixture of cholesteryl ω-(4-hydroxyphenoxy)alkanoate (any

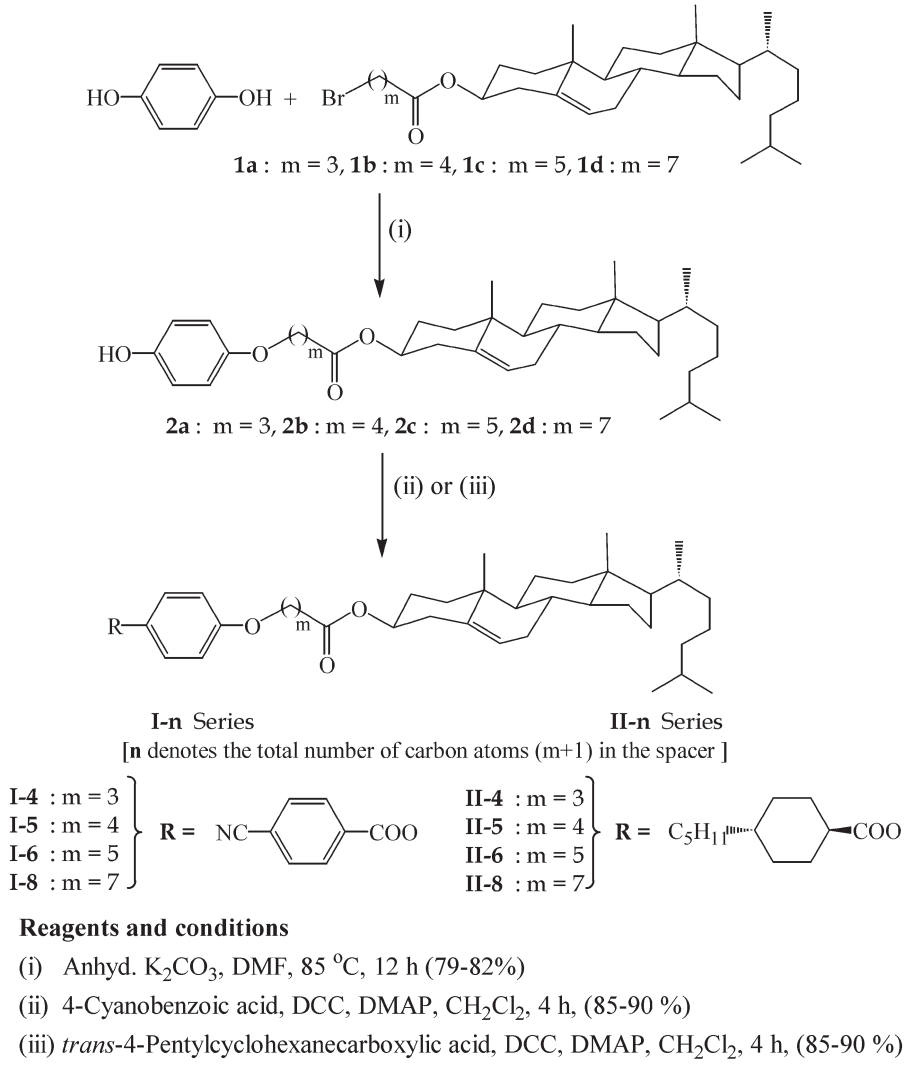

Scheme 1. Synthesis of optically active non-symmetrical dimers.

one among **2a**–**d**) (0.35 mmol, 1 equiv.), 4-cyanobenzoic acid (or *trans*-4-pentylcyclohexanecarboxylic acid) (0.35 mmol, 1 equiv.) and DMAP (0.02 mmol, 0.05 equiv.) in anhydrous CH_2Cl_2 (20 ml) was stirred vigorously for few minutes. To this, a solution of DCC (0.53 mmol, 1.5 equiv.) in dry CH_2Cl_2 (20 ml) was added at room temperature and stirred for 4 h. The white precipitate of *N*,*N*′-dicyclohexylurea was filtered off through a Celite bed. The filtrate was diluted with CH_2Cl_2 (20 ml) and washed with ice-cold 0.5N HCl, saturated Na_2CO_3 solution, water and dried over anhydrous Na_2SO_4. Evaporation of solvent in vacuo furnished the crude product that was purified by column chromatography on neutral alumina using 10% ethyl acetate–hexanes as eluent. The product was recrystallized repeatedly from a CH_2Cl_2:ethanol (1:10) mixture to obtain a white solid.

2.2.2. Cholesteryl ω-[4-(4-cyanobenzoyloxy)phenoxy]-alkanoates (I–n). For **I-4**, R_f=0.48 in 20% EtOAc–hexanes; yield 60%. IR (KBr, cm^{-1}): 2948, 2231, 1730, 1507, 1278, 1194, 1080. UV–vis: λ_{max}=240.9 nm, $\in = 4.37 \times 10^4\,l\,mol^{-1}\,cm^{-1}$. ^1H NMR (400 MHz, $CDCl_3$): δ 8.30 (d, J=6.6 Hz, 2H, Ar), 7.82 (d, J=6.6 Hz, 2H, Ar), 7.12 (d, J=7.1 Hz, 2H, Ar), 6.94 (d, J=7.1 Hz, 2H, Ar), 5.38 (brd, J=3.4 Hz, 1H, 1 × olefinic), 4.65–4.62 (m, 1H, 1 × CHOCO), 4.03 (t, J=4.8 Hz, 2H, 1 × OCH_2), 2.32–1.08 (m, 32H, 6 × CH, 13 × CH_2), 1.02 (s, 3H, 1 × CH_3), 0.92 (d, J=5.2 Hz, 3H, 1 × CH_3), 0.87 (d, J=1.6 Hz, 3H, 1 × CH_3), 0.85 (d, J=1.5 Hz, 3H, 1 × CH_3), 0.67 (s, 3H, 1 × CH_3). MS (FAB+): m/z calcd. for $C_{45}H_{60}NO_5$ (M+1) 694.4, found 695. Elemental analysis: calcd. for $C_{45}H_{59}NO_5$ C 77.88, H 8.57, N 2.02; found C 78.09, H 8.48, N 1.90%.

For **I-5**, R_f=0.49 in 20% EtOAc–hexanes; yield 64%. IR (KBr, cm^{-1}): 2943, 2229, 1738, 1507, 1269, 1192, 1074. UV–vis: λ_{max}=240.9 nm, $\in = 3.81 \times 10^4 l\,mol^{-1}\,cm^{-1}$; ^{1}H NMR (400 MHz, $CDCl_3$): δ 8.30 (d, J=6.6 Hz, 2H, Ar), 7.82 (d, J=6.6 Hz, 2H, Ar), 7.12 (d, J=7.2 Hz, 2H, Ar), 6.94 (d, J=7.2 Hz, 2H, Ar), 5.38 (brd, J=3.4 Hz, 1H, 1 × olefinic), 4.63–4.62 (m, 1H, 1 × CHOCO), 3.98 (t, J=4.4 Hz, 2H, 1 × OCH_2), 2.38–1.08 (m, 34H, 6 × CH, 14 × CH_2), 1.02 (s, 3H, 1 × CH_3), 0.92 (d, J=5.2 Hz, 3H, 1 × CH_3), 0.87 (d, J=1.7 Hz, 3H, 1 × CH_3), 0.85 (d, J=1.7 Hz, 3H, 1 × CH_3), 0.67 (s, 3H, 1 × CH_3). ^{13}C NMR (400 MHz, $CDCl_3$): 172.88, 163.98, 157.04, 143.91, 139.67, 133.55, 132.41, 130.65, 122.72, 122.20, 117.95, 116.94, 115. 21, 73.96, 67.85, 56.71, 56.14, 50.03, 42.34, 39.75, 39.55, 38.19, 37.01, 36.63, 36.21, 35.84, 34.29, 31.94, 31.88, 28.66, 28.28, 28.06, 27.85, 24.33, 23.86, 22.88, 22.62, 21.74, 21.06, 19.38, 18.75, 11.90. MS (FAB+): m/z calcd. for $C_{46}H_{61}NO_5$ 707.5; found 707.9. Elemental analysis: calcd. for $C_{46}H_{61}NO_5$ C 78.04, H 8.68, N 1.98; found C 78.17, H 8.32, N 1.92%.

For **I-6**, R_f=0.52 in 20% EtOAc–hexane; yield 84%. IR (KBr, cm^{-1}): 2946, 2230, 1733, 1510, 1275, 1194, 1081. UV–vis: λ_{max}=240.6 nm, $\in = 3.41 \times 10^4 l\,mol^{-1}\,cm^{-1}$. ^{1}H NMR (400 MHz, $CDCl_3$): δ 8.30 (d, J=6.6 Hz, 2H, Ar), 7.82 (d, J=6.5 Hz, 2H, Ar), 7.12 (d, J=7.2 Hz, 2H, Ar), 6.94 (d, J=7.1 Hz, 2H, Ar), 5.38 (brd, J=3.4 Hz, 1H, 1 × olefinic), 4.63–4.62 (m, 1H, 1 × CHOCO), 3.98 (t, J=5.0 Hz, 2H, 1 × OCH_2), 2.32–1.08 (m, 36H, 6 × CH, 15 × CH_2), 1.02 (s, 3H, 1 × CH_3), 0.92 (d, J=5.2 Hz, 3H, 1 × CH_3), 0.87 (d, J=1.5 Hz, 3H, 1 × CH_3), 0.85 (d, J=1.5 Hz, 3H, 1 × CH_3), 0.67 (s, 3H, 1 × CH_3). MS (FAB+): m/z calcd. for $C_{47}H_{64}NO_5$ (M+1) 722.5; found 722.7. Elemental analysis: calcd. for $C_{47}H_{63}NO_5$, C 78.19, H 8.79, N 1.94; found, C 78.17, H, 9.13, N 1.95%.

For **I-8**, R_f=0.61 in 20% EtOAc–hexane, yield (74%). IR (KBr, cm^{-1}): 2935, 2231, 1737, 1507, 1273, 1175, 1074. UV–vis: λ_{max}=240.8 nm, $\in = 2.70 \times 10^4 l\,mol^{-1}\,cm^{-1}$. ^{1}H NMR (400 MHz, $CDCl_3$): δ 8.30 (d, J=6.7 Hz, 2H, Ar), 7.82 (d, J=6.6 Hz, 2H, Ar), 7.12 (d, J=7.2 Hz, 2H, Ar), 6.94 (d, J=7.2 Hz, 2H, Ar), 5.38 (brd, J=3.4 Hz, 1H, 1 × olefinic), 4.63–4.60 (m, 1H, 1 × CHOCO), 3.97 (t, J=5.2 Hz, 2H, 1 × OCH_2), 2.32–1.08 (m, 40H, 6 × CH, 17 × CH_2), 1.02 (s, 3H, 1 × CH_3), 0.92 (d, J=5.2 Hz, 3H, 1 × CH_3), 0.87 (d, J=1.9 Hz, 3H, 1 × CH_3), 0.86 (d, J=1.7 Hz, 3H, 1 × CH_3), 0.68 (s, 3H, 1 × CH_3). MS (FAB+): m/z calcd. for $C_{49}H_{68}NO_5Na$, 773.5; found 773.5. Elemental analysis: calcd. for $C_{49}H_{67}NO_5$, C 78.46, H 9.00, N 1.87; found, C 78.50, H 9.24, N 1.67%.

2.2.3. Cholesteryl ω-[4-(*trans*-1,4-butylcyclohexanoyloxy)-phenoxy]alkanoates (II-n). For **II-4**, R_f=0.77 in 20% EtOAc–hexane; yield 61%. IR (KBr, cm^{-1}): 2928, 2849, 1742, 1559, 1246, 1194, 1052. UV–vis: λ_{max}=278 nm, $\in = 2.33 \times 10^3 l\,mol^{-1}\,cm^{-1}$. ^{1}H NMR (400 MHz, $CDCl_3$): δ 6.96 (d, J=8.6 Hz, 2H, Ar), 6.86 (d, J=8.6 Hz, 2H, Ar), 5.37 (brd, J=3.6 Hz, 1H, 1 × olefinic), 4.66–4.62 (m, 1H, 1 × CHOCO), 3.99 (t, J=5.8 Hz, 2H, 1 × OCH_2), 2.52–0.67 (m, 68H, 6 × CH_3, 21 × CH_2, 8 × CH). MS (FAB+): m/z calcd. for $C_{49}H_{77}O_5$ (M+1), 745.6; found 745.6. Elemental analysis: calcd for $C_{49}H_{76}O_5$, C 78.98, H 10.28; found, C 79.28, H 10.06%.

For **II-5**, R_f=0.83 in 20% EtOAc–hexanes; yield 58%. IR (KBr, cm^{-1}): 2933, 2860, 1753, 1594, 1247, 1191, 978. UV–vis: λ_{max}=278 nm, $\in = 2.00 \times 10^3 l\,mol^{-1}\,cm^{-1}$. ^{1}H NMR (400 MHz, $CDCl_3$): δ 6.96 (d, J=7.0 Hz, 2H, Ar), 6.86 (d, J=7.0 Hz, 2H, Ar), 5.38 (brd, J=4.3 Hz, 1H, 1 × olefinic), 4.66–4.58 (m, 1H, 1 × CHOCO), 3.97 (t, J=5.8 Hz, 2H, 1 × OCH_2), 2.44–0.67 (m, 70H, 6 × CH_3, 22 × CH_2, 8 × CH). MS (FAB+): m/z calcd. for $C_{50}H_{79}O_5$ (M+1), 759.6; found 759.5. Elemental analysis: calcd. for $C_{50}H_{78}O_5$, C 79.11, H 10.36; found, C 79.20, H 10.30%.

For **II-6**, R_f=0.86 in 20% EtOAc–hexane; yield 68%. IR (KBr, cm^{-1}): 2933, 2848, 1739, 1506, 1248, 1193, 1029. UV–vis: λ_{max}=278.2 nm, $\in = 2.01 \times 10^3 l\,mol^{-1}\,cm^{-1}$. ^{1}H NMR (400 MHz, $CDCl_3$): δ 6.96 (d, J=8.2 Hz, 2H, Ar), 6.86 (d, J=8.6 Hz, 2H, Ar), 5.36 (brd, J=4.3 Hz, 1H, 1 × olefinic), 4.66–4.58 (m, 1H, 1 × CHOCO), 3.94 (t, J=5.9 Hz, 2H, 1 × OCH_2), 2.44–0.67 (m, 72H, 6 × CH_3, 23 × CH_2, 8 × CH). MS (FAB+): m/z calcd. for $C_{51}H_{81}O_5$ (M+1), 773.6; found 773.8. Elemental analysis: calcd. for $C_{51}H_{80}O_5$, C 79.22, H 10.43; found, C 79.48, H 10.72%.

For **II-8**, R_f=0.89 in 20% EtOAc–hexane; yield 75%. IR (KBr, cm^{-1}): 2932, 2853, 1735, 1504, 1245, 1191, 1009. UV–vis: λ_{max}=278.1 nm, $\in = 2.92 \times 10^3 l\,mol^{-1}\,cm^{-1}$. ^{1}H NMR (400 MHz, $CDCl_3$): δ 6.96 (d, J=9.0 Hz, 2H, Ar), 6.86 (d, J=9.0 Hz, 2H, Ar), 5.37 (brd, J=4.2 Hz, 1H, 1 × olefinic), 4.65–4.57 (m, 1H, 1 × CHOCO), 3.93 (t, J=6.4 Hz, 2H, 1 × OCH_2), 2.31–0.67 (m, 76H, 6 × CH_3, 25 × CH_2, 8 × CH). ^{13}C NMR (400 MHz, $CDCl_3$): 175.19, 173.30, 156.67, 144.20, 139.73, 122.65, 122.26, 114.99, 73.75, 68.29, 56.71, 56.14, 50.03, 43.63, 42.34, 39.75, 39.55, 38.19, 37.20, 37.02, 36.95, 36.63, 36.21, 35.84, 34.70, 32.33, 32.20, 31.94, 31.88, 29.22, 29.07, 28.28, 28.06, 27.85, 26.58, 25.90, 25.01, 24.33, 23.86, 22.88, 22.74, 22.62, 21.06, 19.37, 18.75, 14.17, 11.90. MS (FAB+): m/z calcd. for $C_{53}H_{84}O_5$, 800.6; found 799.4. Elemental analysis: calcd for $C_{53}H_{84}O_5$, C 79.45, H 10.57; found, C 79.16, H 10.27%.

3. Results and discussion

3.1. *Mesomorphic properties*

Two rod-like cores differing in their structural features were employed to synthesize two series of cholesterol-based dimers, **I-n** and **II-n**, enabling a comparative study. In both types of compounds, the length and

Table 1. Phase sequence, transition temperatures (°C) and enthalpies ($J\,g^{-1}$, in square brackets) for the non-symmetrical chiral dimers synthesized. (Cr=crystal; TGBC*=twist grain boundary phase with SmC* blocks; TGB=twist grain boundary phase with SmA or SmC blocks; I=isotropic liquid).

Dimer	Heating (Cooling)
I-4	Cr 120.8 [50.3] SmA 201.5[a] TGB[b] N* 224.6 [5.6] I (I 218.5 [5.3] N* 200.4[a] TGB[b] SmA 89.4[c] Cr)
I-5	Cr 108.6 [14.6] SmA 159.1 [1.0][d] TGB[b] N* 179.1 [2] I (I 175.9 [1.9] N* 154.7 [0.9][d] TGB[b] SmA 94.8[c] Cr)
I-6	Cr 84.2 [15.8] SmA 178.2[a] TGB[b] N* 212.7 [5.4] I (I 208 [5.2] N* 177.1[a] TGB[b] SmA 58.6[a] SmC* 53.8[c] Cr)
I-8	Cr 96 [14.5] SmA 148.5[a] TGB[b] N* 187.2 [5.7] I (I 182.5 [5.6] N* 145.9[a] TGB[b] SmA 66.5[c] Cr)
II-4	Cr 126.4 [35.1] SmA 163.4[a] TGB 167.5[a] N* 210 [4.5] I (I 209.5 [4.5] N* 167[a] TGB 162.1[a] SmA 110.2[a] TGBC* 101.2 [26] Cr)
II-5	Cr 94.8 [28] N* 157.3 [1.5] I (I 154.4 [1.4] N* 52.4[c] Cr)
II-6	Cr 94.6 [20.1] TGBC* 133.8[a] N* 190 [4.8] I (I 187.2 [4.5] N* 133.1[a] TGBC* 64.8[c] Cr)
II-8	Cr 136 [37.8] N* 174 [4.7] I (I 168.1 [4.7] N* 81[c] Cr)

[a]Phase transition observed by POM; too weak for recognition by DSC. [b]A transient enantiotropic phase. [c]Crystallization observed only by POM. [d]Enthalpy is the combined enthalpy of the SmA–TGB and TGB–N* transitions.

parity of the ω-oxyalkanoyl spacer has been varied to reveal its effect on the mesomorphism within the series. Phase sequences, transition temperatures and associated enthalpies for all the dimers are summarized in table 1. Phase transition temperatures were determined by a combination of POM and DSC measurements. Peak temperatures in DSC thermograms obtained during the first heating and cooling cycles at $5^{\circ}C\,min^{-1}$ were combined with optically measured temperatures. Transition enthalpies were derived from DSC measurements.

It can be seen from table 1 that the chiral dimers of the **I-n** series, which have a phenyl 4-cyanobenzoate core, exhibit a polymesomorphic sequence. In particular, dimers **I-4**, **I-5** and **I-8** possessing an 4-oxybutanoyl (C_4), 5-oxypentanoyl (C_5), and 8-oxyoctanoyl (C_8) spacer, respectively, exhibit enantiotropic SmA, TGB and N* mesophases, whereas dimer **I-6** with an 6-oxyhexanoyl (C_6) spacer also stabilizes a monotropic SmC* phase. POM study of these samples, placed between a pair of ordinary glass slides, revealed that they exhibit a focal-conic texture on cooling from the isotropic (I) phase. When subjected to mechanical stress, the focal-conic pattern transforms to a planar texture coexisting with a fingerprint pattern, as shown in figure 1 a; these textures are characteristics of the N* phase and the occurrence of the fingerprint pattern indicates that the pitch of the helix

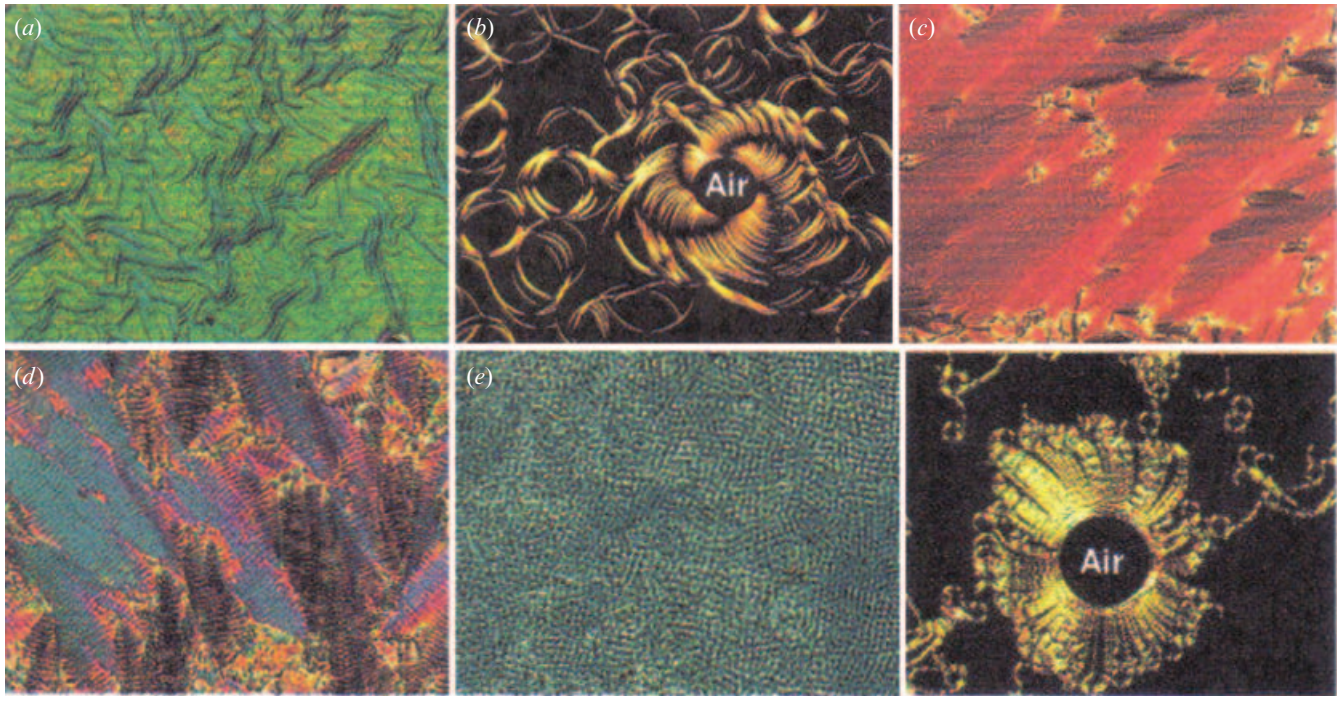

Figure 1. Microphotographs of the different mesophases of the chiral dimers: (a) N* (at 205°C), (b) TGB, and SmA (at 140°C) phases of **I-4**; (d) SmC* phase (at 55°C) of **I-6**; (e) planar and (f) homeotropic TGBC* phase (at 106°C) of **II-4**.

is quite large. On cooling the N* phase, a TGB phase having either SmA or(SmC blocks, appears over a very short temperature interval before transforming into the SmA phase. The TGB phase showed the usual filament as well as planar textures; the former type of pattern was seen (figure 1 b) exclusively when substrates treated for homeotropic alignment were used. The SmA phase showed a focal-conic fan coexistent with a pseudoisotropic texture. The occurrence of the SmA was further evidenced based on the observation of focal-conic fan pattern (figure 1 c) in slides treated for planar orientation and a dark field of view in slides treated for homeotropic orientation. The structure of the SmA phase stabilized by these compounds may not differ significantly from earlier reports that cholesterol-based dimers having polar terminal group form an interdigitated SmA structure [7, 13], as discussed earlier. The stabilization of the SmC* phase in dimer **I-6** was evident as it showed the banded focal-conic and cloudy textures on cooling the coexistent focal-conic and pseudoisotropic patterns of the SmA phase, respectively. Indeed, when slides treated for homogeneous alignment were used a partially aligned (broken) focal conic fan texture with dechiralization lines on top of it was observed solely, as shown in figure 1 d.

A plot of the clearing temperature as a function of the total number of carbon atoms **n** in the flexible spacer (figure 2) shows a typical odd–even alternating curve. However, the variation in the length and parity of the spacer does not seem to influence on the mesomorphic behaviour of these compounds since they show nearly identical phase sequences.

Of the four dimers of the **II-n** series, the first member, **II-4** with a 4-oxybutanoyl (C_4) spacer, stabilizes enantiotropic SmA, TGB and N* phases in addition to a metastable TGBC* phase. The existence of the TGBC* was confirmed based on the textural observation. When the sample was cooled from the homogeneously aligned SmA phase (with focal-conic texture), a mesophase appears at 110°C with a slightly blurred planar texture (difficult to focus) initially, which quickly transforms to square grid pattern, as shown in figure 1 e. If the plates are treated for homeotropic alignment then undulated filaments grow (figure 1 f) over the pseudo-isotropic pattern of the SmA phase; all these features confirm the presence of the TGBC* phase. Dimer **II-6** with a 6-oxyhexanoyl (C_6) spacer stabilizes an enantiotropic TGBC* phase below the N* phase; on cooling this dimer from the planar pattern of N* phase, the TGBC* phase displayed the characteristic square grid pattern. It is worth mentioning here that several fascinating structures are likely for the TGBC* phase owing to the local SmC* tilt of the molecules [24–27]. Nonetheless, the occurrence of the square grid pattern for planar anchoring condition seems to be a good evidence for the TGBC* structure proposed by Renn [25] in which, in addition to the occurrence of a helical superstructure due to the TGB helix, the SmC* blocks exhibit the director helix of the bulk SmC* phase, with the helix axis perpendicular to that of the TGB helix. Another structure has been proposed for this phase to which the authors refer to as undulated TGBC* (UTGBC*) phase owing to the undulated nature of the smectic layers [27]. Experimentally it has been found that the TGBC* or UTGBC* phase exhibits a square grid pattern superimposed on the planar texture as expected. Interestingly, Clark and co-workers have recently demonstrated that these features arise from a common structure: ''giant'' smectic blocks of planar layers terminated by grain boundaries [28]. On the other hand, compounds **II-5** and **II-8** of the series were evidenced to show the N* phase only. In this series also the clearing temperature of the dimers exhibits a prominent dependence on parity of the spacer. The variation in the length and parity of the spacer also seems to influence the mesomorphic behaviour of these compounds to some extent.

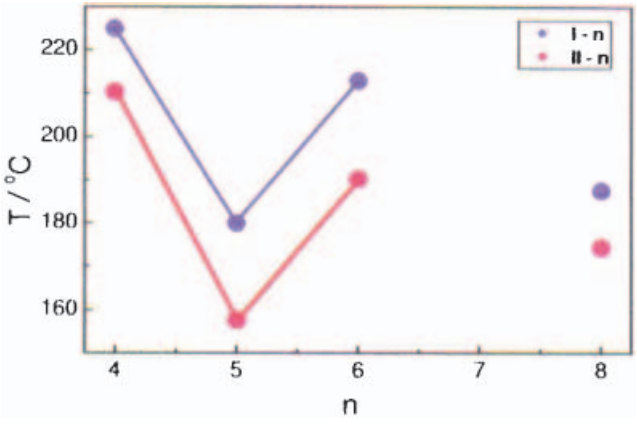

Figure 2. Influence of the number of carbon atoms, **n** (m+1), in the ω-oxyalkanoyl spacer on the clearing temperature for the **I-n** and **II-n** series.

From these results, it can be seen that the dimers of the **I-n** series with a phenyl 4-cyanobenzoate core display a polymesomorphic sequence, whereas compounds belonging to the **II-n** series possessing phenyl *trans*-4-pentylcyclohexanecarboxylate unit do not support such a behaviour. Thus, our studies show that the nature and extent of mesomorphism are quite sensitive to the structure of the achiral rod-like mesogen attached to the cholesterol unit through polymethylene spacers. In general, the dimers comprising an even-parity spacer display a well ordered N* phase, leading to a higher N*–I transition as well as higher enthalpy value.

3.2. *Optical properties of the chiral nematic phase*

The N* phase is well known to display several unique optical properties [22, 24, 29–30] and, thus, has received considerable attention since its discovery [24]. In a well aligned planar sample, the nematic-like layers within the N* phase are slightly twisted from one another forming a macroscopic helical (chiral) structure with a pitch length *p*; this is the basis for the unique optical properties, i.e. selective reflection and the optical activity (optical rotation) of the phase. If the pitch length of the N* phase is of the order of the wavelength of incident visible light, then colours are selectively reflected. In general, the selective reflection wavelength depends on the molecular chirality and ordering of the molecules within the phase. Importantly, the helical pitch is temperature-dependant and thus, the colour of the reflected light varies with temperature, a feature that has been well used in temperature-sensing device applications. From this viewpoint, cholesterol-based non-symmetrical dimers are promising given the fact that they provide several distinctive ways of modulating the selective reflection wavelength of the N* phase by changing the parity of the spacer [11, 12, 14] and/or by substituting them with a photoresponsive core [22]. For example, recent investigations by Marcelis *et al.* [11, 12, 14] and Tamaoki and co-workers [22] on such dimers have shown that the selective reflection wavelength of the N* phase displays an odd-even effect as a function of the parity of the interlinking spacer. In fact, Luckhurst and co-workers have also reported analogous results for chiral dimers without cholesterol entity [31]. Remarkably, photolysis of the supercooled N* phase formed by dimers comprising cholesterol-azobenzene leads to a hypsochromic shift (decrease) in the reflected wavelength indicating that the pitch of the helical structure can be photo controlled.

In view of these observations, we investigated the optical properties of the N* phase stabilized by these dimers. The temperature dependence of selective reflection was measured with the help of UV–vis–NIR scanning spectrophotometer coupled with a programmable hot stage. The substance held between two quartz plates was heated to its isotropic phase, and cooled slowly. The N* phase formed was sheared to obtain Grandjean (planar) texture in which the helix of the phase becomes normal to the quartz plates and the structure reflects the incident light. Figure 3 shows the dependence of the selective reflection wavelength (measured from the transmission spectra) on the temperature of N* phase obtained during cooling cycles for dimers **I-4, I-6** and **I-8**. It can be seen that for these dimers the wavelength of selective reflection is relatively higher in agreement with earlier reports that the dimers with even-parity spacer reflect at a higher wavelength which can be attributed to

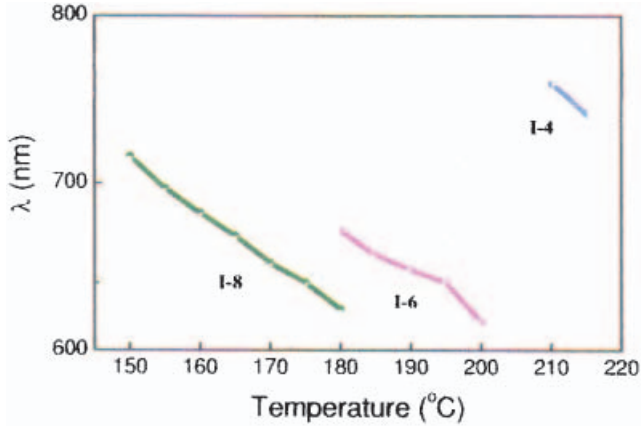

Figure 3. Dependence of the selective reflection wavelength on temperature of the N* phase observed in the cooling cycle of dimers of the **I-n** series.

different (higher) ordering of the molecules in the N* phase [11, 12, 14, 22, 31]. All the three dimers exhibit a bathochromic (red) shift with decrease in temperature, as summarized in table 2. On the other hand, the reflection wavelengths of the N* phase for **I-5** could not be measured as it did not show any prominent transmittance peak above 360 nm indicating that its helical pitch length falls below this wavelength. Indeed, some detectable peaks seen in this region possibly arise due to the presence of aromatic rings.

As expected, the N* phase of dimers of **II-n** series, i.e. **II-4**, **II-6** and **II-8** with an even-parity spacer, selectively reflected the light at higher wavelengths (550–780 nm) (figure 4). In these compounds also, the reflection wavelength shifts gradually to the higher side upon decreasing the temperature of N* phase (see table 3). For compound **II-5** with 5-oxypentanoyl (C_5) spacer, no peaks were seen until about 110°C, although below this temperature the prominent reflection bands were obtained with initial red shift followed by shorter wavelength (hypsochromic) shift on lowering the temperature of N* phase. The selective reflection bands observed in this temperature range can be attributed to the, the higher ordering of the N* phase as a function of temperature.

In order to investigate the chiroptical property of the N* phase [29, 32], circular dichroism (CD) measurements were carried out for all the dimers. It is well known that due to macroscopic helical structure, the N* phase exhibits CD phenomenon wherein the incident light is resolved into its two circularly polarized components, left and right, at a given wavelength. At this wavelength, depending upon the helical sense (chirality) of the phase, circularly polarized light of a particular handedness is completely reflected, whereas

Table 2. Temperature-dependent UV and circular dichroism (CD) data for the N* phase of series **I-n** dimers.

			CD	
Dimer	Temperature/°C	UV-vis λ_{max}/nm	λ_{max}/nm	CD signal/mdeg
I-4	215	741	751, 320	142, −88
	210	757	754, 326	16, −36
I-5	165	–	352, 452	151, 70
	160	–	354, 466	196, 91
	155	–	354, 466	219, 12
I-6	200	616	588, 331, 254	40.3, −21, −0.2
	195	639	590, 333, 253	74.5, −31, −3
	190	647	606, 331, 253	87.9, −34, −10
	185	656	608, 330, 253	98.1, −30, −24
	180	670	625, 366, 328, 254	101, 26, −29, −35
I-8	180	624	595, 313, 261	875, −161, −53
	175	640	596, 312, 261	827, −155, −65
	170	651	599, 308, 261	880, −160, −77
	165	668	604, 351, 309, 261	823, 256, −166, −85
	160	681	619, 352, 309, 261	766, 256, −182, −107
	155	696	641, 353, 310, 261	752, 298, −198, −107
	150	715	655, 353, 309, 261	731, 346, −220, −113

its counterpart is transmitted. Thus, the selective reflection of circularly polarized light of one sense at chiral nematic pitch band should nearly correspond to the one obtained in the UV–vis spectrum. The thin films of the substances prepared during the selective reflection measurement by UV–vis spectroscopic method were employed for this study. It must be mentioned here that, unlike the N* phase, the CD phenomenon was immeasurably small for the isotropic phase. This implies that the chromophores are not influenced by the molecular chirality, but they are affected by the chirality of the phase. The temperature dependence of the CD spectra recorded in the entire N* phase range for the all the dimers of **I-n** and **II-n** are shown in figures 5 and 6, respectively.

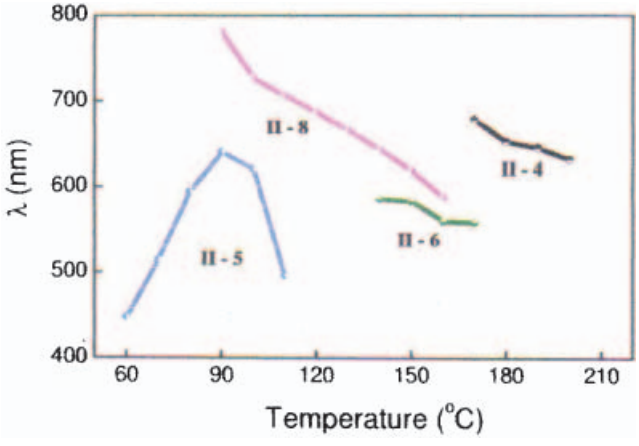

Figure 4. Dependence of the selective reflection wavelength on temperature of the N* phase observed in the cooling cycle of dimers of the **II-n** series.

As can be seen in figure 5, the dimers **I-4**, **I-6** and **I-8** each show broad positive bands in the range of 580 to 755 nm, the intensity of which generally increases (except in some cases) with decreasing temperature, as

Table 3. Temperature-dependent UV and CD data for the N* phase of series **II-n** dimers.

			CD	
Dimer	Temperature/ °C	UV-vis λ_{max}/nm	λ_{max}/nm	CD signal/mdeg
II-4	200	631	594, 291, 246	201, 70, −58
	190	645	550, 290, 248	600, 298, −275
	180	652	876, 290, 248	606, 332, −343
	170	678	959, 289, 247	608, 336, 382
II-5	150	–	306, 269, 247	1901, 124, −57
	140	–	304, 267, 247	158, 102, −25
	130	–	308, 266, 246	655, 92, −5
	120	–	312, 267, 248	379, 69, −7
	110	494	486, 270, 248	45, 29, −29
	100	619	627, 274, 248	42, 28, −40
	90	638	647, 273, 248	51, 29, −44
	80	592	605, 271, 248	45, 29, −43
	70	512	517, 271, 248	42, 29, −37
	60	446	473, 270, 246	286, 39, −28
I-6	170	557	559, 280, 250	1234, 115, −251
	160	558	570, 281, 250	734, 108, −235
	150	581	584, 279, 250	410, 107, −235
	140	584	598, 278, 249	228, 111, −239
I-8	160	585	565, 281, 242	146, 35, −99
	150	616	599, 281, 243	148, 34, −101
	140	641	630, 281, 243	142, 35, −100
	130	664	655, 283, 244	159, 36, −103
	120	685	674, 281, 244	162, 36, −110
	110	704	685, 281, 245	170, 37, −119
	100	725	701, 281, 244	173, 40, −126
	90	779	731, 280, 243	147, 42, −137

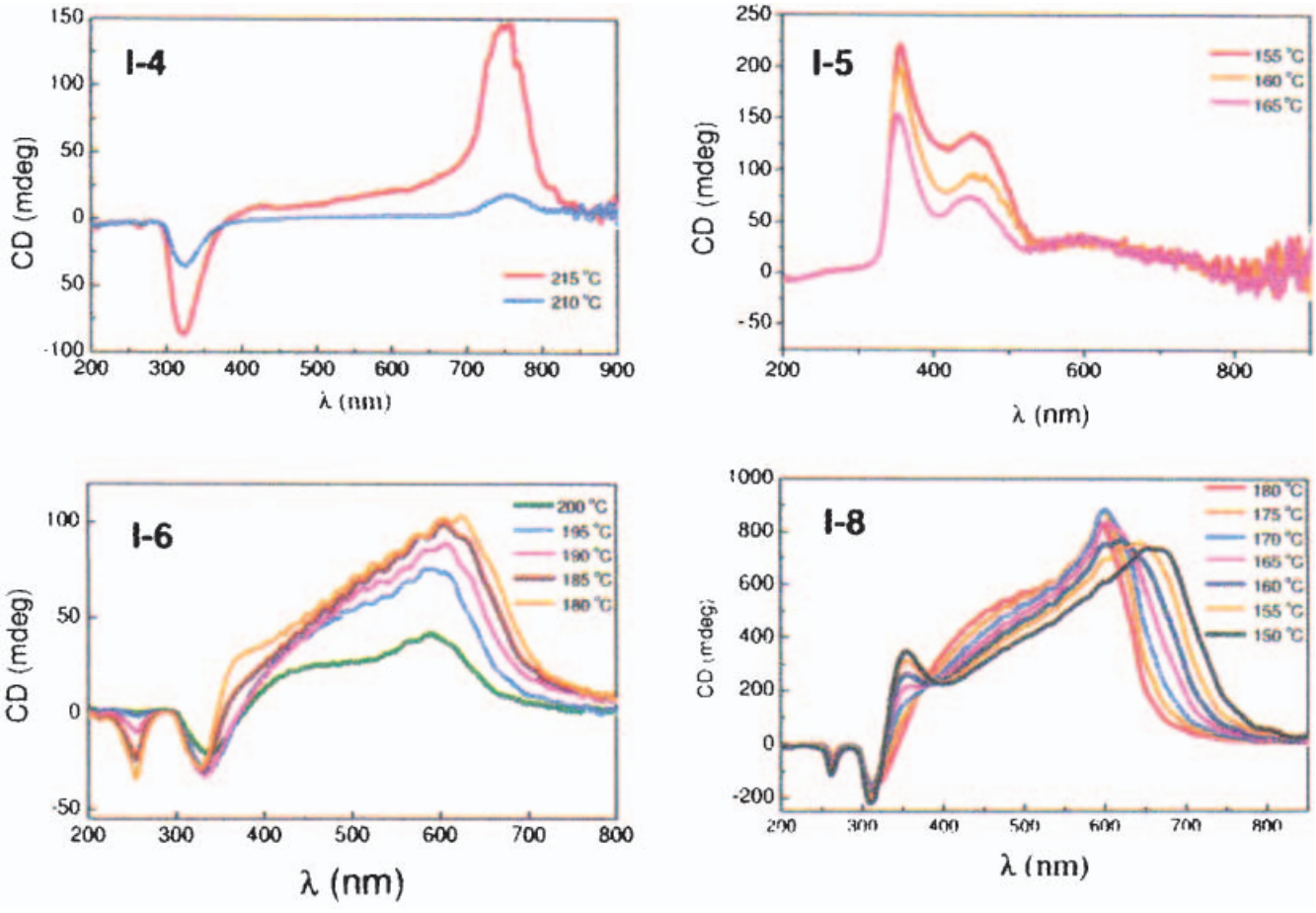

Figure 5. Dependence of the CD spectra on temperature of the N* phase observed in the cooling cycle of dimers of the **I-n** series.

summarized in table 2. These CD transitions can be attributed to the selective reflection wavelengths of circularly polarized light by the helical structure of the phase and are relatively close to the ones obtained in UV spectra. Dimer **I-4** shows a negative band, whereas **I-6** displays two negative bands below 350 nm. Interestingly, **I-8** possesses one positive and two negative bands. In all the cases, the transitions occurring in these regions can be assigned to the circular dichroism of chromophores and phenyl rings. Analogous results have been reported; in particular, the sign of the CD bands in the aromatic cores is observed to be opposite to that of the selective reflection (pitch)-band CD of the N* phase [32].

The CD spectra of even-members belonging to **II-n** series show a positive broad prominent band at the longer wavelength region (>400 nm) that must be originating from the selective reflection (figure 6). In addition, these spectra showed less intense positive and negative bands at shorter wavelength side (<300 nm) that can be assigned to the CD of chromophores and phenyl ring. For dimer **II-5** some interesting features were observed in the CD spectra. A strong positive peak (at about 300 nm) with a weak shoulder (at about 270 nm) was seen in each of the CD spectra obtained at temperatures above 110°C. This positive band vanishes on lowering the temperature further; instead, a broad peak appears above 450 nm whose wavelength is comparable to that of the UV–vis spectra (see figure 6 and table 3). Therefore, the origin of these bands can be assigned to the selective light reflection by the N* phase. This indicates that at lower temperatures the pitch of the N* helix of **II-5** is comparable to the one formed by dimers having even-parity spacer. In other words, it may be reasonable to imagine that this compound attains rod-like molecular conformation in the N* phase when temperature is lowered. Furthermore, all the spectra showed a weak negative CD signal at about 246 nm that can be assigned to CD of aromatic rings. Thus, chiroptical measurement in the N* phase by CD formally indicate its optically active (helical) supramolecular macroscopic organization in which intermolecular interactions between electronic transitions occur. It is also be pointed out here that the positive pitch band observed indicates right-handed screw sense of the chiral nematic

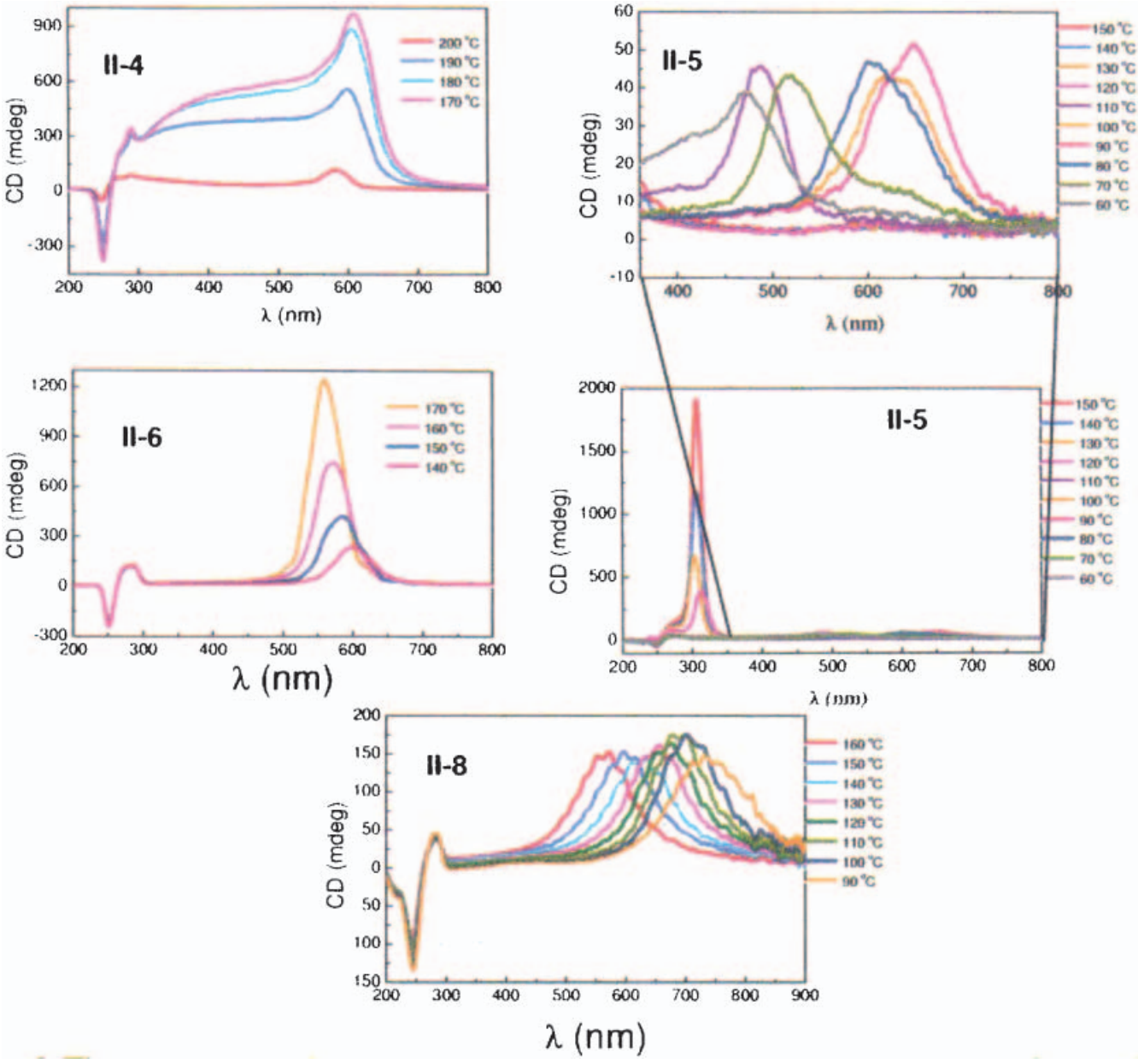

Figure 6. Dependence of the CD spectra on temperature of the N* phase observed in the cooling cycle of dimers of the **II-n** series.

structure which is in accordance with the fact that most steroidal ester are right-handed.

4. Summary

In this paper, we have reported the synthesis and liquid crystallinity of two varieties of optically active non-symmetric dimers in which cholesterol has been linked to either phenyl 4-cyanobenzoate or phenyl cyclohexane-carboxylate cores through a flexible spacer. The dimers with terminal cyano group exhibit a polymesomorphic behaviour; they display chiral nematic, twist grain boundary and smectic A phases with an optional smectic C* phase. However, compounds containing an *n*-pentyl tail stabilize N* with or without twist grain boundary phase possessing the SmC* blocks. The expected odd–even effect was observed within each series. Thus, the phase sequences and clearing temperatures of these set of dimers are dependant on the structure of the ''second mesogen'' attached to the cholesterol and spacer parity. UV–vis and CD spectroscopy were carried out in the neat chiral nematic phase. Analogous to earlier reports, an odd–even effect was observed for the selective reflection wavelengths measured for both the series of dimers. To

the best of our knowledge, this is the first elaborative study on the chiroptical property of the chiral nematic phase formed by non-symmetric chiral dimers. The present investigation could facilitate further understanding of the structure–property relationships cholesterol-based non-symmetrical dimers.

Acknowledgement

We thank Dr. S. Krishna Prasad for his interest in this work and helpful discussions.

References

[1] (a) C.T. Imrie, G.R. Luckhurst. *Handbook of Liquid Crystals,* Vol. 2B, D. Demus, J.W. Goodby, G.W. Gray, H.-W. Spiess, V. Vill (Eds). Part III, p. 799, Weiley-VCH, Germany (1998); (b) C.T. Imrie, P.A. Henderson. *Curr. Opin. Colloid Interface Sci*., **7**, 298 (2002); (c) C.T. Imrie. In *Structure and Bonding - Liquid Crystal II*, D.M.P. Mingos (Ed), p. 149, Springer-Verlag (1999).
[2] F. Hardouin, M.F. Achard, J.-I. Jin, J.W. Shin, Y.K. Yun. *J. Phys., Paris II*, **4**, 627 (1994).
[3] F. Hardouin, M.F. Achard, J.-I. Jin, Y.K. Yun. *J. Phys., Paris II*, **5**, 927 (1995).
[4] F. Hardouin, M.F. Achard, J.-I. Jin, Y.K. Yun, S.J. Chung. *Eur. Phys. J. B*, **1**, 47 (1998).
[5] S.-W. Cha, J.-I. Jin, M. Laguerre, M.F. Achard, F. Hardouin. *Liq. Cryst.*, **26**, 1325 (1999).
[6] F. Hardouin, M.F. Achard, M. Laguerre, J.-I. Jin, D.H. Ko. *Liq. Cryst.*, **26**, 755 (1999).
[7] D.W. Lee, J.-I. Jin, M. Laguerre, M.F. Achard, F. Hardouin. *Liq. Cryst.*, **27**, 145 (2000).
[8] S.-W. Cha, J.-I. Jin, M.F. Achard, F. Hardouin. *Liq. Cryst.*, **29**, 755 (2002).
[9] J.-W. Lee, Y. Park, J.-I. Jin, M.F. Achard, F. Hardouin. *J. Mater. Chem.*, **13**, 1367 (2003).
[10] K.-N. Kim, E.-D. Do, Y.-W. Kwon, J.-I. Jin. *Liq. Cryst.*, **32**, 229 (2005).
[11] A.T.M. Marcelis, A. Koudijs, E.J.R. Sudholter. *Recl. Trav. Chim. Pays-Bas*, **113**, 524 (1994).
[12] A.T.M. Marcelis, A. Koudijs, E.J.R. Sudholter. *Liq. Cryst.*, **18**, 843 (1995).
[13] A.T.M. Marcelis, A. Koudijs, E.A. Klop, E.J.R. Sudholter. *Liq. Cryst.*, **28**, 881 (2001) and references cited therein.
[14] A.T.M. Marcelis, A. Koudijs, Z. Karczmarzyk, E.J.R. Sudholter. *Liq. Cryst.*, **30**, 1357 (2003).
[15] V. Surendranath. *Mol. Cryst. liq. Cryst.*, **332**, 135 (1999).
[16] (a) C.V. Yelamaggad, A. Srikrishna, D.S. Shankar Rao, S.K. Prasad. *Liq. Cryst.*, **26**, 1547 (1999); (b) C.V. Yelamaggad. *Mol. Cryst. liq. Cryst*. **326**, 149 (1999).
[17] C.V. Yelamaggad, S.A. Nagamani, D.S. Shankar Rao, S.K. Prasad, U.S. Hiremath. *Mol. Cryst. liq. Cryst.*, **363**, 1 (2001).
[18] (a) C.V. Yelamaggad, U.S. Hiremath, D.S. Shankar Rao. *Liq. Cryst.*, **28**, 351 (2001); (b) D.S. Shankar Rao, S. Krishna Prasad, V.N. Raja, C.V. Yelamaggad, S. Anitha Nagamani. *Phys. Rev. Lett*., **87**, 085540 (2001); (c) C.V. Yelamaggad, S.A. Nagamani, U.S. Hiremath, G.G. Nair. *Liq. Cryst*., **28**, 1009 (2001); (d) C.V. Yelamaggad, M. Mathews. *Liq. Cryst*., **30**, 125 (2003).
[19] C.V. Yelamaggad, I. Shashikala, Uma S. Hiremath, D.S. Shankar Rao, S. Krishna Prasad. *Liq. Cryst.*, **34**, 153 (2007).
[20] W.-K. Lee, K.-N. Kim, M.F. Achard, J.-I. Jin. *J. Mater. Chem.*, **16**, 2289 (2006) and references cited therein (2006).
[21] (a) C.V. Yelamaggad, A.S. Achalkumar, N.L. Bonde, A.K. Prajapati. *Chem. Mater.*, **18**, 1076 (2006); (b) C.V. Yelamaggad, I. Shashikala, G. Liao, D.S. Shankar Rao, S. Krishna Prasad, Q. Li, A. Jakli. *Chem. Mater*., **18**, 6100 (2006).
[22] (a) V. Ajay Mallia, N. Tamaoki. *Chem. Soc. Rev.*, **33**, 76 (2004) and references cited therein. (b) V. Ajay Mallia, N. Tamaoki. *J. Mater. Chem*. **13**, 219 (2003).
[23] (a) P.J. Shannon. *Macromolecules*, **16**, 1677 (1983); (b) I.W. Hamley, C. Castelletto, P. Parras, Z.B. Lu, C.T. Imrie, T. Itoh. *Soft Matter*, **1**, 355 (2003).
[24] H.-S. Kitzerow. In *Chirality in Liquid Crystals*, H.-S. Kitzerow, C. Bahr (Eds), Springer-Verlag New York (2001).
[25] S.R. Renn. *Phys. Rev. A.* **45**, 953 (1992).
[26] (a) W. Kuczynski, H. Stegemeyer. *Mol. Cryst. liq. Cryst.*, **260**, 377 (1995); (b) W. Kuczynski, H. Stegemeyer. *Proc. SPIE, Int. Soc. Opt. Edn.*, **3318**, 90 (1997).
[27] P.A. Pramod, R. Pratibha, N.V. Madhusudana. *Curr. Sci.*, **73**, 761 (1997).
[28] J. Fernsler, L. Hough, R.-F. Shao, J.E. Maclennan, L. Navailles, M. Brunet, N.V. Madhusudana, O. Mondain-Monval, C. Boyer, J. Zasadzinski, J.A. Rego, D.M. Walba, N.A. Clark. *PNAS*, **102**, 14191 (2005).
[29] S. Chandrasekhar. *Liquid Crystals* second edn, Cambridge University Press, Cambridge (1992).
[30] (a) B. Bahadur. *Liquid Crystals: Applications and Uses.* Vol. 1–3, World Scientific, Singapore (1990); (b) F. Reinitzer. *Monatsh*., **9**, 421 (1888).
[31] A.E. Blatch, I.D. Fletcher, G.R. Luckhurst. *J. Mater. Chem.* **7**, 9 (1997).
[32] (a) F.D. Saeva, J.J. Wysocki. *J. Am. chem. Soc.*, **93**, 5928 (1971); (b) F.D. Saeva, G.R. Olin. *J. Am. chem. Soc*., **95**, 7882 (1973); (c) H. Toriumi, I. Uematsu. *Mol. Cryst. liq. Cryst*. **116**, 21 (1984); (d) H. Toriumi, K. Yahagi, I. Uematsu. *Mol. Cryst. liq. Cryst*. **116**, 21 (1984); (e) M. Sisido, R. Kishi. *Macromolecules*, **24**, 4110, (1991); (f) D.K. Rout, S.P. Barman, S.K. Pulapura, R.A. Gross. *Macromolecules*, **27**, 2945 (1994).